Desalination and Water Treatment
www.deswater.com

doi: 10.5004/dwt.2021.26851

216 (2021) 326–337
March

Corresponding relationship between microorganism propagation and coagulation behavior of a hybrid fruit-peel coagulant

Ying Fu*, Xiangjun Meng

School of Civil Engineering and Architecture, University of Jinan, Shandong, Jinan 250022, China, Tel. +(86)15863798335; emails: cea_fuy@ujn.edu.cn (Y. Fu), mxj_tmjzxy@163.com (X.J. Meng)

Received 12 May 2020; Accepted 27 November 2020

ABSTRACT

A hybrid fruit-peel (HFP) coagulant and its antiseptic modifier (AHFP) were prepared from the peels of banana and orange, and the coagulation behavior in treating simulated both humic acid (HA) water and clay water was studied. The changes in bacterial growth and propagation (BGP) with increasing standing time was probed with UV-vis spectrophotometer (UV), anthrone–sulfuric acid method, potassium dichromate method, pH meter, potentiometer, optical microscope, and diluted-coating plate method, respectively. The results indicated the coagulation performance and parameters characterizing the BGP of HFP and AHFP all experienced some declining and rising cycles (DRCs) with the increasing of standing time (turbidity removal by HFP and AHFP from 96.7% at 0 d to 69% at 8 d to 49.8% at 32 d to 59.5% at 45 d and to 87.6% at 50 d, and from 95% at 0 d to 57.9% at 31 d, to 86.1% at 36 d, to 56.4% at 45 d, and to 76% at 50 d, respectively), but the coagulation performance did not always show a good corresponding relationship with the BGP. AHFP posed a strong adaptability to water qualities. HFP and AHFP were negatively charged. The BGP in HFP was rapidly (densely dispersed filaments or short lines with large size microorganisms appeared at 6 d), while the BGP in AHFP was slowly (only a small number of dispersed agglomerates appeared at 6 d). HFP gave better stability in colony number than AHFP. HFP and AHFP posed a complex co-coagulation or superposition action conducted by microorganisms and natural organic polymers (NOPs), in which the neutralization action was small.

Keywords: Banana peel; Orange peel; Standing time; Microorganisms; Natural organic polymers (NOPs); Coagulation behavior; Corresponding relationship

1. Introduction

With the increasing global population and improving people living standards, the amount of solid waste increases sharply. The daily output of solid waste will reach 11 million tons by the end of this century on the earth [1,2], in which organic solid waste accounts for the largest proportion. Agricultural and forestry waste (AFW) is one of the organic solid wastes [2,3]. Especially in China, AFW pollution is even less optimistic due to the rapid development of AFW industries [4]. As one of recycling natural resources, more and more researches on the AFW value has been carried out in the past 20 y, in which the resource treatment has attracted more and more attention [5,6]. As one of the natural polymer substances, AFW contains a large amount of nontoxic cellulose and saccharide [7,8], therefore, AFW has received worldwide attention in the field of water and wastewater treatment in recent years, in which the researchers are increasingly concerned about developing natural polymer coagulants [9,10]. Compared with inorganic coagulants [11–14], natural polymer coagulants having the unique characteristics of easy biodegradation have lots of advantages in the application of water treatment: abundant raw materials, low price, large selectivity,

* Corresponding author.

safety, biodegradability, and no secondary pollution, especially the sludge formed during water treatment can be reused in farmland, but natural polymer coagulants gave instability and short storing time. As a large category of AFW, fruit peel is extremely prone to be mildewed and has been one of increasing pollution sources [15], which makes it a huge challenge for municipal waste management [16]. The yields of a banana peel or orange peel are huge, in which the former represents about 30%–50% of the total fruit weight of banana [17] and the latter accounts for 25%–40% of the total fruit weight of an orange. Banana peel and orange peel are all composed of pectin, cellulose, hemicellulose, and lignin which are all functional ingredients of coagulants, moreover, these functional ingredients contain a large amount of active groups (such as hydroxyl and carboxyl) which can be combined with the impurities by chelating, coordinating, complexing, hydrogen bonding, and other actions, giving high application value for water treatment. So the resource utilization of fruit peel has gradually become a research hotspot [18–20]. Banana peel and orange peel are rich in organic carbon and have adsorption properties, so, its current applications in the field of water and wastewater treatment at home and abroad mainly include adsorption [21–23] and direct utilization. For example, as an adsorbent, the peel is to remove heavy metals, nitrogen, phosphorus, oil, and other pollutants, or as a raw material for biochar [24], it is used in agriculture, environment, energy, and waste treatment. But very few studies focused on the preparation of coagulants from fruit peel [25].

In addition, there is also another kind of ecological friendly coagulant–microorganism type [26] which is characterized by non-toxic and harmless, highly active, having no secondary pollution, and a wide range of application. The main working components in microorganism coagulants include the cell itself (such as certain bacteria, yeasts, actinomycetes, etc.) [27–29], cell extracts (proteins or glycans), or metabolites (extracellular polysaccharides, lipids, protein, etc.) [30], in which the extracellular polymeric substance (EPS) is the most functional and the most effective category and has been extensively studied. The active substance exerting coagulation in EPS is generally sodium alginate, cellulose, chitin, starch, xanthan gum, pullulan, etc. These unique characteristics and advantages make microorganism coagulants give promising prospects in water and wastewater treatment [31], so, it is still very attractive for this type of coagulants in application and promotion [26,32]. However, there are still some disadvantages that existed in microorganism coagulants, such as higher cost, lower yield, immature production process, and instability in terms of preparation, storage, or use.

NOPs are the food source of microorganisms. The coagulants prepared from banana peel and orange peel in this work are essentially a kind of NOPs, so, they will be attacked by microorganisms during standing, which is also the basic reason why they gave instability and short storage time. It will be of great significance if the NOPs can be combined with microorganisms to develop a non-toxic and efficient integrated coagulant under well-controlled synthesis and storage conditions. As inferred previously [25], the coagulation performance of banana peel coagulant was a comprehensive action of both NOPs and microorganisms, rather than an individual effect of one kind of composition (NOPs or microorganisms), however, little research has been done on the change of microorganisms in this type of coagulants during standing [25]. Therefore, the research about the relationship between the microorganism change and coagulation behavior of HFP and AHFP during the standing period was mainly conducted in this work.

In this work, a hybrid fruit-peel (HFP) coagulant was prepared using banana peel and orange peel as the main materials, and then was modified by an antiseptic stabilizer to prepare an antiseptic (AHFP) coagulant. This work studied the impact of standing time on coagulation performance of HFP and AHFP in treating both simulated HA water and clay water using Jar tests, and also probed the changes in bacterial concentration, organic matters, total glycans and pH, zeta potential, and microorganism appearance of HFP and AHFP during standing process, respectively. This work is to provide some basic data for the further upgrade preparation and practical application of this type of coagulants, and to open up a new idea for the development and research of an integrated coagulant composed of NOPs and microorganisms.

2. Materials and methods

2.1. Preparation of HFP and AHFP

2.1.1. Preparation of HFP

Step 1: Some dry banana peel from banana (planted in Hainan, China) and dry orange peel from orange (planted in Guangdong, China) were obtained after natural drying 1–2 d at room temperature and then further dried in oven at 70°C for 24 h using GZX-9140MBE electric heat forced air drying oven (Shanghai Boxun, China). The two types of dry peel were finally smashed with CS-700 high speed multi-function pulverizer (COSUAI/Chaoshuai, Zhejiang, China) to make the two peel powders.

Step 2: Some of the two peel powders passed through mesh screen with 100 meshes to obtain the banana sifted substance and orange sifted substance, and then one part of the former was mixed with three parts of the latter to obtain a mixed powder. 0.1 kg mixed powder was added to 4 L tap water (pH = 8.14–8.46, turbidity = 0.12–0.85 NTU, color < 5, and COD_{Mn} = 1.38–2.23 mg/L) under medium stirring for 1–2 min at room temperature, followed by a 10 min standing to obtain an original mixture.

Step 3: 32 mL NaOH (5 mol/L, industrial grade, Tianjin, China) was added to the original mixture under rapid stirring 3 min at room temperature, and was followed by a 10 min water bath at 60°C to obtain a leaching solution. The leaching solution was filtrated with qualitative filter paper (Tianjin, China) to obtain HFP coagulant (stored for 0 d) with pH = 10.79, density = 0.996 g/mL, w (saccharides) = 70.33%, and w (mixed powder) = 27.2 mg/L, respectively. HFP was sealed with adhesive tape and stored at 25°C.

2.1.2. Preparation of AHFP

0.06% highly effective antiseptic stabilizer of 1-2 benzisothiazolin-3-one (C_7H_5NOS, BIT-20) (industrial grade) was added to the HFP coagulant (prepared in section 2.1.1

(preparation of HFP)) under medium stirring 3 min at room temperature, and then was followed by a 2–3 h standing to obtain a AHFP coagulant (stored for 0 d) with pH 10.82. AHFP was sealed with adhesive tape and also stored at 25°C.

HFP and AHFP samples taken out at different standing time from 0 to 50 d were used as coagulants for the following tests.

2.2. Impact of standing time on coagulation behavior of HFP and AHFP

2.2.1. Test water

Simulated humic acid (HA) water and simulated clay water were used as the test water samples.

2.2.1.1. Preparation of simulated HA water

First, a kaolin stock solution and a HA stock solution were prepared. 1 g of HA was dissolved in 0.01 mol/L NaOH solution under stirring 2 h and then was followed by a filtration through 0.45 μm filters (FuZhou LanLo Filtration Equipment Co., Ltd., China) to obtain a HA stock solution with concentration of 1 g/L, which was stored below 4°C before using. 15 g of Kaolin was added to 1 L deionized water under stirring 2 h and was allowed to stand for 3 h, and then the supernatant was taken out as the Kaolin stock solution and was stirred 5 min again just before using. 430 ± 5 mL Kaolin stock solution and 410 ± 5 mL HA stock solution were added to 18 L tap water under medium stirring. After a 15 min stirring, the simulated HA water was obtained with the following qualities: turbidity = 32.1–52.5 NTU, color = 0.276–0.357 A, UV_{254} = 0.204–0.357 cm^{-1}, COD_{Cr} = 14.4–30 mg/L, pH = 7.08–8.46, and temperature = 7°C–15°C.

2.2.1.2. Preparation of simulated clay water

A certain amount of clay was naturally dried at room temperature and then was passed through mesh screen with 100 mesh to obtain a sifted substance. 100 g sifted substance was added to 1 L tap water under medium stirring 30 min, followed by 15 min standing, and 0.8 L supernatant was taken out as clay stock solution. 1.8 L clay stock solution was added to 6 L tap water to obtain mixture water, and then 1.8 g soluble starch, 3 g ammonium chloride, and 0.36 g potassium dihydrogen phosphate were added to the mixture water under medium stirring 15 min to obtain the simulated clay water with the following qualities: turbidity = 111–237 NTU, color = 0.328–0.663 A, UV_{254} = 0.044–0.079 cm^{-1}, COD_{Cr} = 200–348 mg/L, pH = 7.32–7.65, and temperature = 7°C–15°C.

2.2.2. Jar test

The Jar test was performed using a Jar test apparatus (ZR4-6 flocculator, China). The dosage of HFP and AHFP was selected as 30 mg/L based on the previous tests. The standard Jar test procedure consisted of a rapid mix at 200 rpm for 1 min after coagulant addition, and was followed by a 10 and 5 min mixing period at 60 and 40 rpm, respectively. Then the flocs were allowed to settle for 15 min, and the supernatants were then withdrawn from a position of 2–3 cm below the surface for the measurement of turbidity, color, and UV_{254} by HACH 2100 turbidity meter (USA, HACH) and UV-5800 spectrophotometer (Shanghai, China), respectively. Three runs were performed in this test, and the results represented the averages of the tests, and the error bars referred to the standard error of the mean of the three experiments.

The removal of some conventional parameters in coagulation test was only studied in this paper. The removal of other parameters (such as total organic carbon (TOC), biodegradable organic carbon (BOC), total nitrogen (TN), total phosphorous (TP), etc.) will be carried out in the subsequent work.

2.3. Impact of standing time on BGP in HFP and AHFP

2.3.1. Bacterial concentration

The absorbance of HFP and AHFP diluted 10-folds was measured at 600 nm with UV-5800 spectrophotometer (Shanghai, China), as optical density (OD) indicating bacterial concentration. Three runs were performed in this test, and the results represented the averages of the tests, and the error bars referred to the standard error of the mean of the three experiments.

2.3.2. NOPs, total glycans, pH, and zeta potential

2.3.2.1. Natural organic polymers

5 mL of HFP and 5 mL AHFP taken out at the different standing time were centrifuged 10 min (9,000 rpm and 25°C) using Hermle Z 326 K high-speed refrigerated centrifuge (Hermle, Germany), respectively. Then 1 mL supernatant taken out was diluted 50-fold for NOPs measurement with potassium dichromate method.

2.3.2.2. Total glycans

The centrifugation method was the same as that in NOPs. 0.5 mL supernatant taken out after centrifugation was diluted 100-fold, and then 1 mL was taken out for total glycans measurement with anthrone–sulfuric acid method.

2.3.2.3. PH

The pH values of HFP and AHFP at the different standing time were analyzed with S210-S benchtop pH meter (Mettler-Toledo, Switzerland). Each sample was tested in parallel three times and the results represented the averages of the tests, and the error bars referred to the standard error of the mean of the three experiments.

2.3.2.4. Zeta potential

The chargeability of HFP and AHFP at different standing time diluted to 770-folds was analyzed with zetasizer nano particle size potentiometer (Malvin Instruments Co., Ltd.). Each sample was tested three times in parallel and the results represented the averages of the tests, and the error bars referred to the standard error of the mean of the three experiments.

2.3.3. Bacterial morphology and appearance in HFP and AHFP

2.3.3.1. Bacterial morphology

20 μL of HFP and AHFP at different standing time was put on the glass slide and then was photographed with OLYMPUS CX31 optical microscope (Ruike Zhongyi, Beijing) under magnification times of 100.

2.3.3.2. Colony appearance and number

The colonies produced in HFP and AHFP were observed by diluted-coating plate method based on GB/T4789.2-2010. The required items (test tubes, Petri dishes, nutrient agar medium, etc.) were sterilized in MLS-3751L-PC pressure steam sterilizer (Panasonic, Japan) for 20 min at 121°C, and the medium was added to the petri dish with a diameter 90 mm. Lastly, HFP and AHFP taken out at the different standing time were diluted different folds, and then was added to the medium, followed by cultivation 36 h at 36°C and then was photographed.

3. Results and discussion

3.1. Influence of standing time on HFP and AHFP coagulation performance

Figs. 1 and 2 present the changes in coagulation performance by HFP and AHFP in treating simulated both HA water and clay water with the increasing of standing time from 1 to 50 d.

As seen in Figs. 1a and b, HFP at 0 d basically gave the same removal of both turbidity (95%–96.7%) and color (86.4%–88.9%) as AHFP at 0 d, and also posed the similar removal trend of both turbidity and color having some declining and rising cycles (DRCs) with the increasing of standing time. During the standing process, the following two inferences could be obtained. (1) If only NOPs or microorganisms played a role in coagulation action in HFP or AHFP, the reduction in coagulation behavior indicated that the amount or structure of NOPs was reduced or destroyed by the attack of microorganisms, while the recovery of the coagulation behavior indicated that the microorganisms may have played a role in coagulation. (2) If it was not NOP alone or microorganisms that played a role in the coagulation action of HFP or AHFP, then the reduction and recovery of coagulation performance did not have the corresponding relationship with the change in the amount of either NOPs or microorganisms. As to which inference ((1) or (2)) was correct, it needed to be analyzed based on the following component changes in coagulants.

Fig. 1c shows that UV_{254} removal first rose and then decreased, and was followed by a fluctuation within a certain range, but almost above 40%. The removal of UV_{254} did not give a certain corresponding relationship with turbidity removal, indicating that this type of coagulant probably

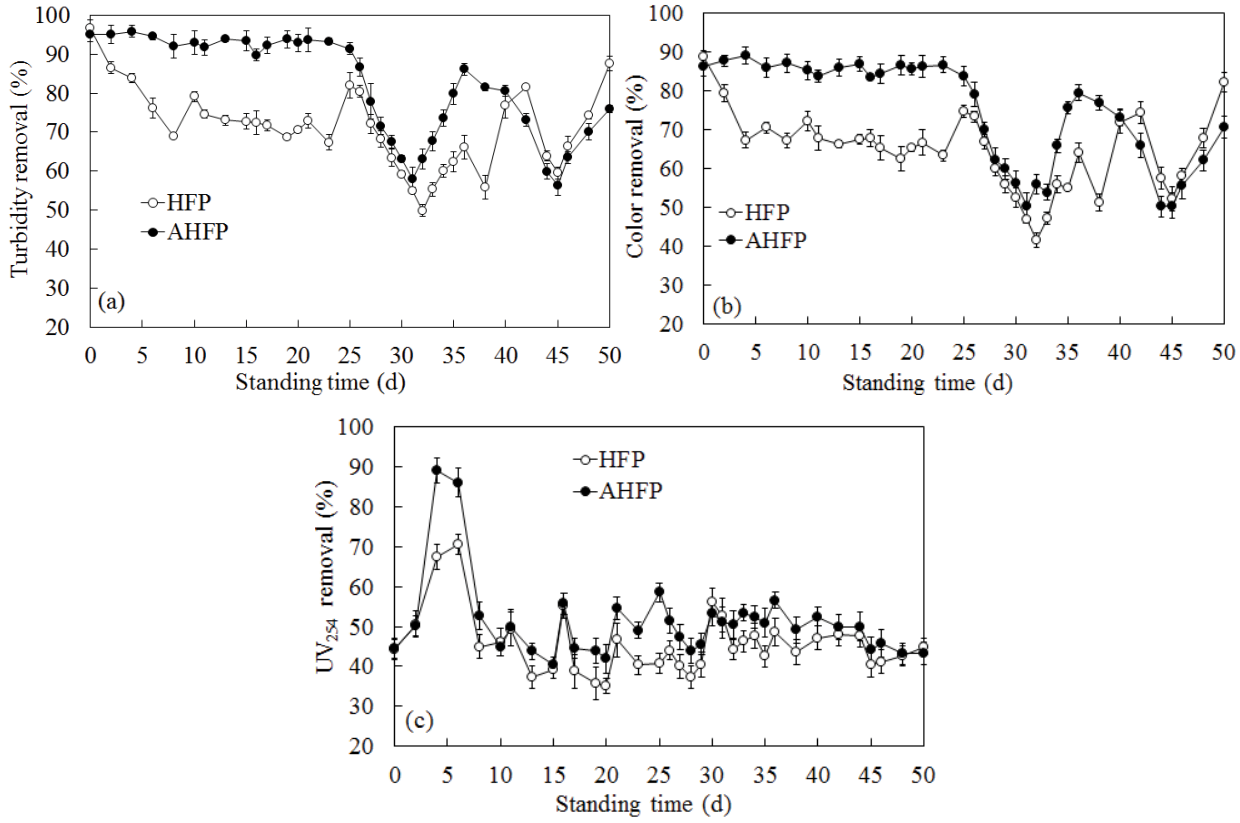

Fig. 1. Impact of standing time on coagulation performance of HFP and AHFP in treating simulated HA water. (a) Turbidity removal (%), (b) color removal (%), and (c) UV_{254} removal (%).

posed different mechanisms in terms of turbidity removal and organic matter removal, and that this kind of coagulant was attributed to organic substance having a tendency to release itself to the water samples, thus probably achieving a dynamic equilibrium of the organic substance in flocs (formed by coagulant and impurities) and in water samples.

For HFP, turbidity, and color removal began to decrease sharply for the first time at 2 d, decreasing by 27.7% and 21.5% at 8 d, respectively, and then was followed by a rebound and decrease again. HFP gave the lowest turbidity and color removal of 49.8% and 41.6% at 32 d, respectively, and then rose again to 87.6% and 82.2% at 50 d, basically similar to that at 2 d. While for AHFP, the first sharp drop was at 26 d, reaching the lowest turbidity and color removal of 57.9% and 50.4% at 31 d, respectively, rebounding and decreasing again, and then was followed by rising again, up to 76% and 70.7% at 50 d, respectively. As seen in Figs. 1a and b, the removal of turbidity by HFP only maintained over 90% within 2 d, compared within 25 d by AHFP. However, AHFP gave both higher turbidity and color removal than HFP at the lowest value in the coagulation process, while giving lower performance than HFP at 50 d again, indicating that the addition of antiseptic stabilizer greatly changed the microbial growth curve, and also changed the ratio of NOPs to microorganisms.

Fig. 2 displays a similar DRCs trend as Fig. 1, but, both the inflection point time of DRCs and the decreasing values of coagulation performance were slightly different. For HFP, the coagulation performance also began to drop sharply for the first time at 2 d, giving the lowest turbidity and color removal of 23.7% and 14.6% at 16 d, respectively, and was followed by rebound, decrease and rise again, rising up to 80.7% and 71.8% at 50 d, basically again back to the similar values at 2 d. The changing magnitude of coagulation behavior in treating the simulated clay water was much larger than that in treating the simulated HA water during the entire standing period. While for AHFP, the first sharp decrease occurred at 25 d, reaching the lowest turbidity and color removal of 58% and 49.3% at 31 d, respectively, and then was followed by rebound, decrease and rise again, and rising again up to 69.8% and 60.5% at 50 d, respectively.

Fig. 2c shows that the removal of UV_{254} by HFP was basically similar to that by AHFP, all showing a DCRs trend. However, the removal of UV_{254} presented negative values: HFP and AHFP were attributed to NOPs, so, the process of treating the simulated clay water by them was actually a process of releasing dissolved organic substance to the water samples.

As seen in Figs. 1 and 2, HFP gave a large difference of DRCs and coagulation performance in treating the simulated clay water from that in treating the simulated HA

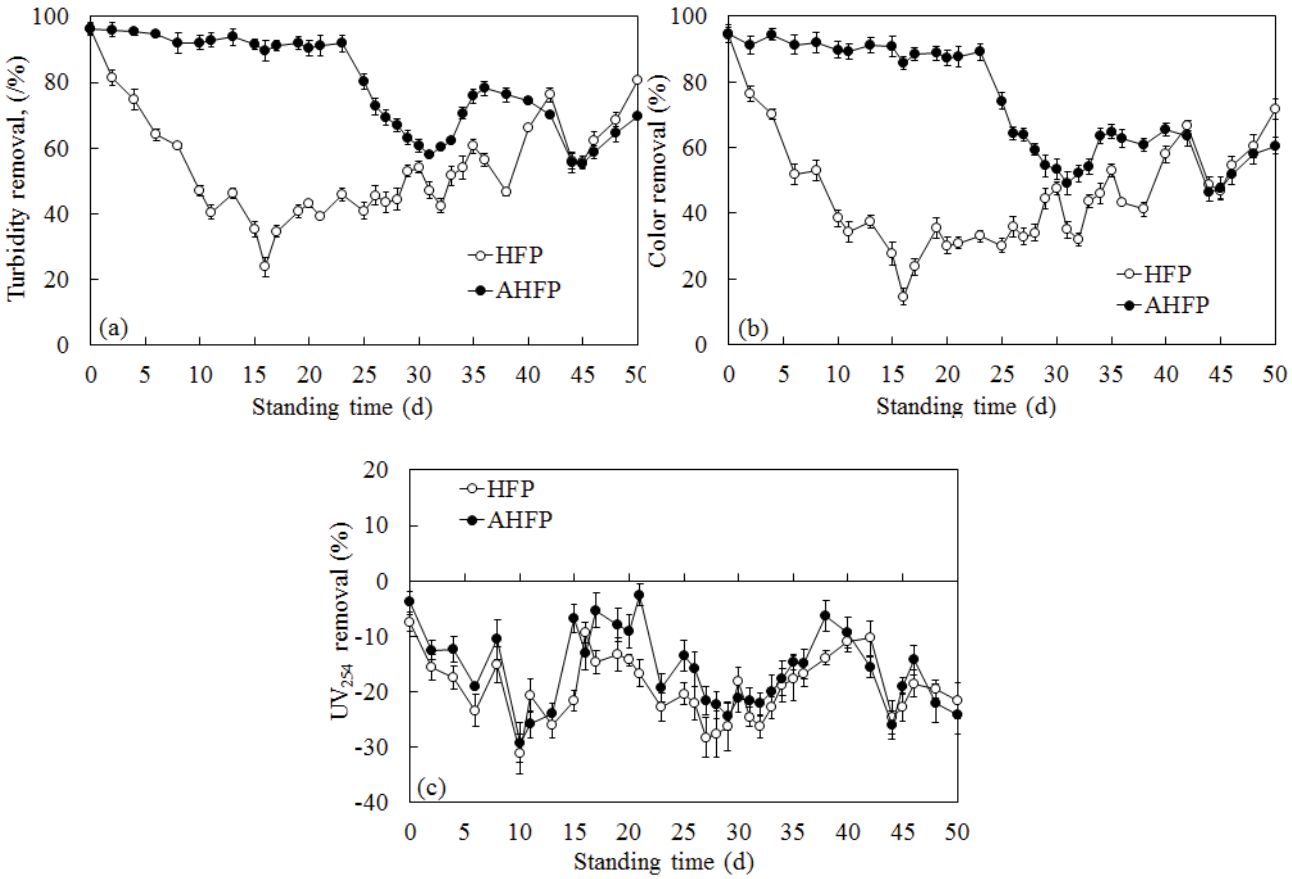

Fig. 2. Impact of standing time on coagulation performance of HFP and AHFP in treating simulated clay water. (a) Turbidity removal (%), (b) color removal (%), and (c) UV_{254} removal (%).

water, in comparison with a smaller difference by AHFP, indicating that AHFP posed a stronger adaptability to water qualities and better stability in removing turbidity and color. In addition, for water samples having higher organic matters, HFP and AHFP further increased dissolved organic matters in the treated water, which provides a possibility for the following idea: HFP or AHFP maybe will become additional slow-releasing carbon source in treating low-carbon source wastewaters, worthy of further study.

3.2. Influence of standing time on BGP in HFP and AHFP

3.2.1. Influence of standing time on change in bacterial concentration

Fig. 3a presents the changes in bacterial concentration (OD) in HFP and AHFP with standing time ranged between 1 and 50 d.

The microbial growth curve includes lag phase, log, stationary, and decline which can be basically inferred from OD values. As shown in Fig. 3a, AHFP gave different length of each phase in BGP from HFP. The lag phase in HFP was very short, almost only lasted 2 d (from 0 to 2 d), and then was followed by a relatively slow log phase (the increment of OD was only 1.68 during this phase). After that, the BGP in HFP entered a relatively stable stationary at 11 d, up to the end of the experimental period. Both log and stationary phase in HFP were all composed of some shorter decline and log phases, suggesting that the microorganisms gave very complicated changes during the entire standing process. While AHFP gave a long lag phase (0–23 d), with OD ranged between 0.44 and 0.66, which was the basic reason for which AHFP almost gave higher coagulation performance within a longer time of standing. After that, the BGP in AHFP entered the fast-growing log phase (23–25 d), with OD rapidly up to 2.15, and then was followed by a slow growth and propagation period, log phase again, and finally the stationary phase.

During the entire experimental period, the OD of HFP had many decline phases with many shorter periods, compared with relatively stable OD of AHFP, moreover, AHFP had a relatively more regular microbial growth curve than HFP. The OD of AHFP was lower than that of HFP before 37 d, and then greater than that of HFP, based on which the relative changes in microbial biomass in HFP and AHFP can be basically inferred. The ratio of OD_{HFP} to OD_{AHFP} was calculated from Fig. 3a, shown in Fig. 3b. This ratio increased rapidly before 25 d, and decreased sharply at 24–25 d, indicating that the amount of bacteria produced by HFP was much larger than that of AHFP at this stage. Then this ratio entered a slow declining, basically fluctuating around 1, indicating that HFP almost gave the similar amount of bacteria to AHFP, but, the number of bacteria in AHFP was slightly larger than that in HFP at in the final stage of this experiment.

The OD of HFP entered a relatively stable period around 11 d (Fig. 3a), but the turbidity and color removal experienced twice big rising in this stable period (Figs. 1 and 2), for example, for simulated HA water, the turbidity removal increased from 49.8% at 32 d to 81.6% at 42 d, and from 59.5% at 45 d to 87.6% at 50 d, respectively, indicating that the ratio of microorganisms to NOPs has changed greatly and that the coagulation behavior was a coordination action of microorganisms and NOPs, instead of single microbial action or NOPs action, which was consistent with the inference (2) in section 3.1 (influence of standing time on HFP and AHFP coagulation performance), and also further confirmed the previous research results [24]. While AHFP gave more than 91% turbidity removal before 25 d, almost corresponding to the lag phase and rapid log phase of the microorganisms. After that, the turbidity removal did not have a complete correspondence with the OD. So, like HFP, the coagulation behavior of AHFP was also a coordination action of microorganisms and NOPs, and also conformed to the inference (2) in section 3.1 (influence of standing time on HFP and AHFP coagulation performance).

3.2.2. Influence of standing time on changes in NOPs, total glycans, pH, and zeta potential

Fig. 4 presents the changes in NOPs (Fig. 4a), total glycans (Fig. 4b), pH (Fig. 4c), and zeta potential (Fig. 4d) of HFP and AHFP with standing time ranged from 1 to 50 d, respectively. Generally, BGP will make NOPs, total glycans, and pH decrease to some extent, by which the BGP situation could be inferred to a certain extent. Zeta

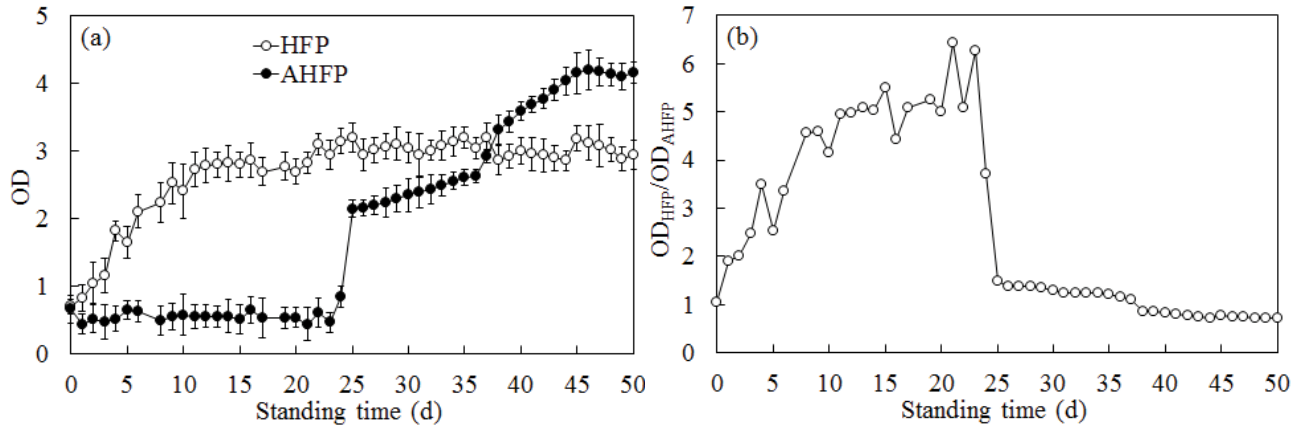

Fig. 3. Impact of standing time on bacterial concentration in HFP and AHFP: (a) OD and (b) OD_{HFP}/OD_{AHFP}.

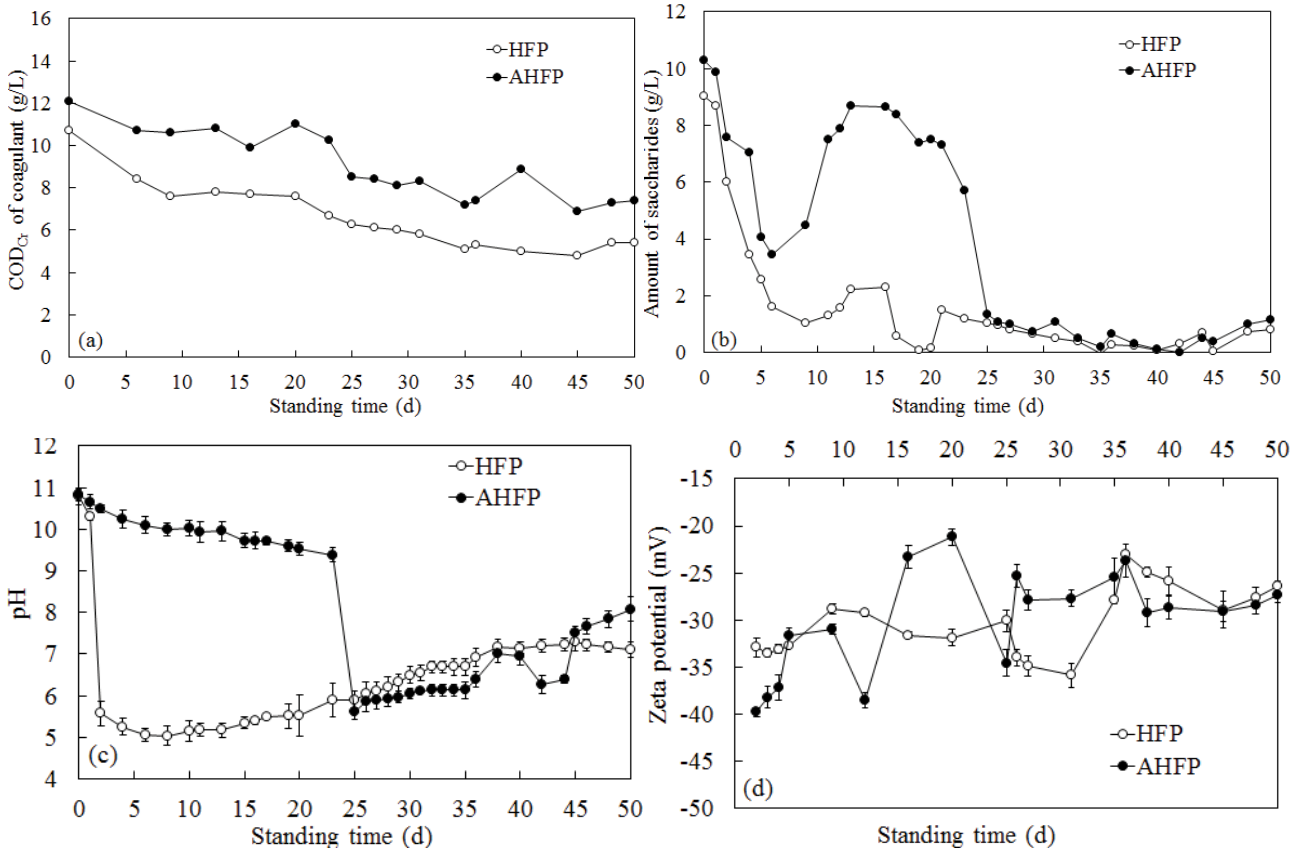

Fig. 4. Impact of standing time on (a) NOPs, (b) total glycans, (c) pH, and (d) zeta potential of HFP and AHFP. NOPs, natural organic polymers.

potential (Fig. 4d) was analyzed after 770-folds dilution of the coagulants, which had practical analytical significance because this dilution folds was almost similar to the dilution folds of coagulant (890-folds) after added to the water samples in Figs. 1 and 2.

As seen from Fig. 4a, the amount of NOPs in AHFP was higher than that in HFP during the entire experiment period, indicating that the destruction of NOPs structure by microorganisms in HFP was more serious than that in AHFP due to the addition of an antiseptic stabilizer to AHFP. For HFP, the amount of NOPs began to decline sharply for the first time at the beginning of the standing, then showed the DRCs, reaching the lowest value at 45 d, and then rose again and tended to be stable. During this process, the declining of coagulation behavior (Figs. 1 and 2) basically corresponded to the NOPs decreasing stage, while the increasing phase of behavior almost corresponded to the NOPs stable stage. This suggested that the NOPs played a very important role in coagulation performance by HFP having no antiseptic stabilizer, thus leading to a decreasing in the coagulation performance when microorganisms destroyed the NOPs structures. The stable phase of NOPs maybe corresponded to the microbial self-consumption phase, in which the microorganisms played a larger coagulation behavior, leading to an increase in coagulation performance, which was basically consistent with the inference (1) in section 3.1 (influence of standing time on HFP and AHFP coagulation performance). In addition, some NOPs changing stages did not give above mentioned corresponding relationships with the coagulation performance, for example, the decline in NOPs at 20 d corresponded to the increasing in coagulation performance, indicating that the coordination or superposition co-coagulation action conducted by microorganisms and NOPs was very complicated, worth further researching.

Like HFP, AHFP also experienced some DRCs, in which the changes in coagulation behavior (Figs. 1 and 2) basically did not correspond to the changes in NOPs, indicating that the addition of antiseptic stabilizer disturbed the relationship between the NOPs structure damage caused by microorganisms and coagulation performance. It further illustrated that the role played by the NOPs in AHFP coagulation was much smaller than that in HFP, and that the coordination or superposition co-coagulation action conducted by microorganisms and NOPs in AHFP was probably always more complicated, which was consistent with the inference (2) in section 3.1 (influence of standing time on HFP and AHFP coagulation performance).

Like coagulation behavior (Figs. 1 and 2), the total glycans also experienced DRCs in HFP and AHFP. For HFP (Fig. 4b), the total glycans decreased sharply for the first time at 2 d, reaching the lowest value of 0.087 g/L at 19 d, and then a little rebound, decrease, and rebound again. The DRCs of total glycans in HFP was similar to an energy

consumption process, in which the energy amplitude gradually decreased. Moreover, the correlation between the decreasing and increasing of the total glycans (Fig. 4b) and turbidity and color removal became smaller with the increasing of standing time, indicating that the coagulation action in HFP was mainly controlled by NOPs if the standing time was short, that is, HFP was a kind of NOPs coagulant at this stage, consistent with the inference (1) in section 3.1 (influence of standing time on HFP and AHFP coagulation performance). With the increasing of standing time, the amount of microorganisms increased in HFP, thus making HFP a coagulant co-existed by NOPs and microorganisms, in which superposition action was strengthened, so consistent with the inference (2) in section 3.1 (influence of standing time on HFP and AHFP coagulation performance). While for AHFP (Fig. 4b), the total glycans also decreased sharply for the first time at 2 d, reaching the lowest point of 0.0017 g/L at 42 d, and then a little rebound. Unlike HFP, the decreasing and increasing of the total glycans (Fig. 4b) in AHFP gave a small correlation with the turbidity and color removal during the entire standing time, indicating that the coagulation action in AHFP was not simply conducted by individual NOPs or individual microorganisms, but a co-coagulation and superposition action consisted of NOPs and microorganisms, consistent with the previous studies [25] and inference (2) in section 3.1 (influence of standing time on HFP and AHFP coagulation performance).

As seen from Fig. 4c, AHFP gave much higher pH than HFP at standing time less than 25 d, and was followed by a slightly lower than HFP at standing time of 25–45 d, and then a little higher than HFP after standing time longer than 45 d, indicating that the BGP in AHFP at early stage was much lower than that in HFP and at a later stage was similar to that in HFP, moreover, further suggesting that the antiseptic stabilizer in AHFP maybe lost its effectiveness at about 25 d. However, the coagulation performance of AHFP (Figs. 1 and 2) had not greatly reduced due to the failure of the antiseptic stabilizer, which further proved that the coagulation performance of AHFP was a coordinated action of microorganisms and NOPs.

As displayed in Fig. 4c, the pH changes in HFP and AHFP also experienced some DRCs, but, the correlation between the DRCs of pH in HFP and coagulation performance was less than that in AHFP. For HFP, the pH dropped sharply for the first time at 2 d, reaching the lowest value 5.04 at 8 d. After that, the pH of HFP experienced a small increase and decrease for a long time. While for AHFP, the pH gave a slightly decreasing in the initial long-time period, from 10.82 at 0 d to 9.38 at 23 d, and then quickly fell to the lowest value at 25 d, and then experienced some DRCs. HFP gave a strong correlation between the pH change and coagulation performance before 8 d, and was followed by a weakened correlation, however, the pH change in AHFP had a smaller correlation with the coagulation performance before 31 d, and was followed by an enhanced correlation. This suggested that only NOPs in HFP conducted coagulation performance in the early stage and a synergistic effect between NOPs and microorganisms played a role in the later stage, and a synergistic effect between NOPs and microorganisms in AHFP was very complicated. This was consistent with the results and inferences of Figs. 4a and b.

As seen from Fig. 4d, both HFP and AHFP were negatively charged, and the pollutants in the water samples treated in this work were also basically negatively charged, so HFP and AHFP almost gave no or only a little neutralization action on pollutants. Therefore, there should be no corresponding relationship between Zeta potential and coagulation behavior, which was consistent to the relationship between Figs. 1 or 2 and 4d. Microbial coagulants are also generally negatively charged. Therefore, if the background NOPs in HFP and AHFP were uncharged or the charge carried by the NOPs was negligible, the change in the charges carried by both microorganisms and their metabolites could be inferred from the change in the charge carried by the coagulants: an increasing in zeta potential indicates a decreasing in the negative charges carried by the microorganisms and their metabolites, indicating that the amount of microbial biomass or its activity decreased, vice versa. As shown from Fig. 4d, the zeta potential also experienced DRCs, but its change degree in HFP was much smaller than that in AHFP, indicating that the microorganism growth and decay cycle or the biomass amount and activity law of microorganisms in AHFP were very different from that in HFP due to the addition of antiseptic stabilizers, which also further affected the ratio of microbial biomass to NOPs or microbial activity cycle (or law). This further proved the reason for which the coagulation performance DRCs by AHFP in Figs. 1 and 2 were significantly different from that in HFP, also further illustrating that this type of coagulant gave a synergy coagulation behavior of NOPs and microorganisms and this coagulation behavior was quite complicated, which was consistent with both the inference of (2) in section 3.1 (influence of standing time on HFP and AHFP coagulation performance) and the inference and analysis in Figs. 3 and 4.

3.2.3. Influence of standing time on bacterial morphology and appearance change in HFP and AHFP

Although the following pictures could not fully show the actual situation of microorganisms, the BGP in HFP and AHFP could also be reflected to some extent.

3.2.3.1. Bacterial morphology

Fig. 5 displays the changes in bacterial morphology of HFP and AHFP with standing time ranged from 1 to 50 d.

As seen in Fig. 5, the bacterial morphology in HFP (Fig. 5a) was very different from that in AHFP (Fig. 5b). The microorganisms in HFP presented to be some densely dispersed filaments or short lines, in comparison with some dispersed microbial masses or aggregates in AHFP. For HFP, the microorganisms grew and propagated rapidly. Some larger-size microorganisms already filled in the liquid at 6 d, and then the microorganism amount increased slightly with the increasing of standing time, and was followed by an agglomerating tendency slightly after 36 d, but the overall changing degree was less than that in AHFP. While for AHFP, the growth and propagation of microorganisms was very slower, although some microbial aggregates also appeared in the liquid at 6 d, the amount was lower, consistent with the previous studies [25]. But the

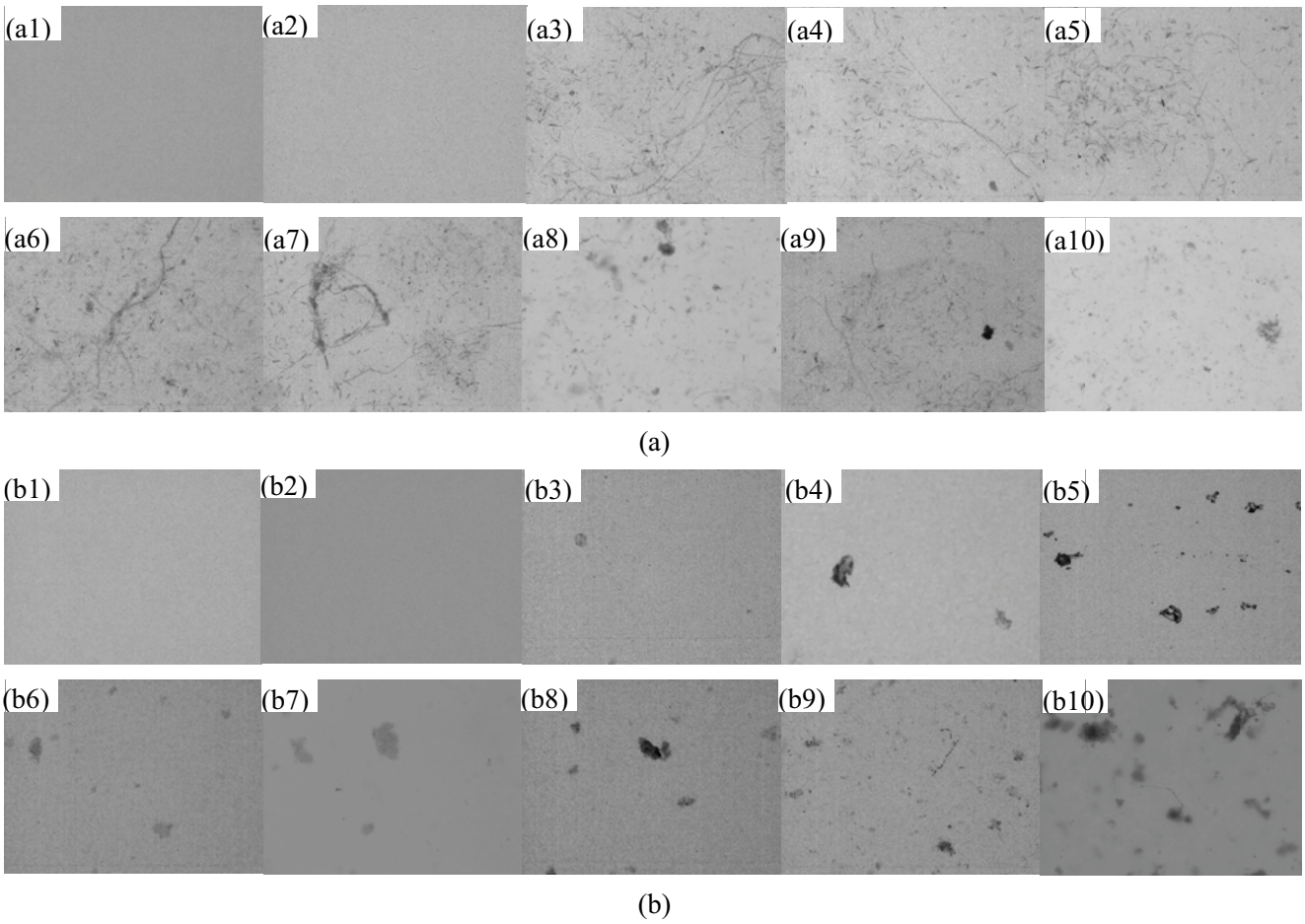

Fig. 5. Impact of standing time on bacterial morphology in (a) HFP (100×) and (b) AHFP (100×). (a1) 0 d, (a2) 2 d, (a3) 6 d, (a4) 12 d, (a5) 16 d, (a6) 25 d, (a7) 31 d, (a8) 36 d, (a9) 44 d, (a10) 50 d; (b1) 0 d, (b2) 2 d, (b3) 6 d, (b4) 12 d, (b5) 16 d, (b6) 25 d, (b7) 31 d, (b8) 36 d, (b9) 44 d, and (b10) 50 d.

color of microorganism aggregates in AHFP became lighter from 25 to 31 d, indicating that the microorganism categories or characteristics probably changed significantly. The influence of microorganisms or their synergy with NOPs on the coagulation behavior could not be judged from the bacterial morphology in Fig. 5.

3.2.3.2. Colonial appearance and number

The determined dilution folds of the coagulants and the number of colonies produced in Fig. 6 were summarized in Table 1 based on the results of some tentative experiments.

The colony number (Table 1) and colony appearance (Fig. 6) in HFP gave great difference from those in AHFP with the increasing of standing time. The colony number (Table 1) of HFP reached 1.18×10^6 at 5 d, compared with 8.5×10^3 in AHFP. AHFP only reached 6.6×10^4 at 24 d, while HFP was already 7.6×10^{12}, during which the number of larger-size colonies in HFP (Table 1 and Fig. 6) increased rapidly, while AHFP colonies tended to shrink in size but probably increased in intensity (Fig. 6). As displayed in section 3.1 (influence of standing time on HFP and AHFP coagulation performance) and 3.2 (influence of standing time on BGP in HFP and AHFP), the parameters characterizing the microorganisms in HFP and AHFP basically changed greatly and coagulation performance also decreased significantly during the period from 23 to 25 d: the bacterial concentration in AHFP (Fig. 4) increased rapidly, NOPs, total glycans, and alkalinity decreased sharply (Fig. 4), the color of microorganisms became lighter (Fig. 5), and the coagulation performance also decreased quickly (Figs. 1 and 2). This indicated that the combination between denser microorganisms with smaller size and NOPs was not suitable for the effective development of coagulation action, which also provided a certain research direction for the future investigation on an integrated coagulant composed of NOPs and microorganisms.

As also displayed in Table 1, after 24 d, the dilution fold of HFP was always 10^{11} and the order of magnitudes of the colonies was between 10^{12} and 10^{13}. While the number of AHFP colonies changed significantly after 24 d, with the order of magnitudes from 10^4 at 24 d to 10^{10} at 31 d, and then to 10^{15} and 10^{14} at 45 d and 50 d, respectively. The changing magnitude of AHFP colony number was significantly larger than that of HFP in the later period, indicating that the dense degree of colonies in the

Table 1
Dilution-folds of coagulants and number of colony produced in HFP and AHFP

Standing time/d		1	5	15	24	31	36	40	45	50
HFP	Dilution folds	10^2	10^4	10^{10}	10^{11}	10^{11}	10^{11}	10^{11}	10^{11}	10^{11}
	Number of colonies/(×dilution folds)	53	118	190	76	108	<310	<90	<180	51
AHFP	Dilution folds	10^2	10^2	10^2	10^3	10^9	10^{10}	10^{12}	10^{13}	10^{13}
	Number of colonies/(×dilution folds)	64	85	110	66	44	<310	<160	<130	60

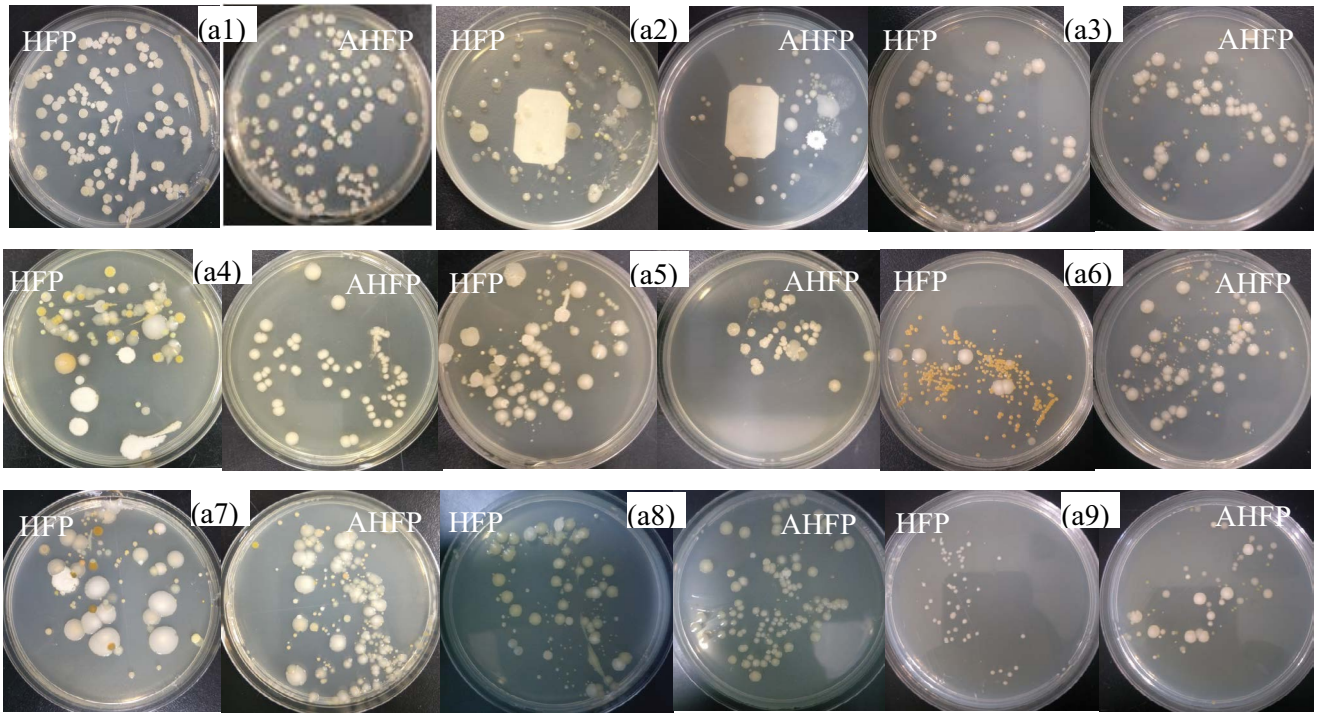

Fig. 6. Impact of standing time on colony apperance and number in HFP and AHFP. (a1) 0 d, (a2) 5 d, (a3) 15 d, (a4) 24 d, (a5) 31 d, (a6) 36 d, (a7) 40 d, (a8) 45 d, and (a9) 50 d.

agglomerated microorganisms in AHFP was quite large (almost consistent with the agglomerated state of microorganisms in Fig. 5), resulting in a larger colony number in AHFP in the later period of standing time than that in HFP. This is basically consistent with the changes in the bacterial concentration ratio of HFP to AHFP (Fig. 3b), NOPs, pH (Fig. 4), and bacterial morphology and amount (Fig. 5): HFP gave a relatively stable change, compared with a great fluctuation in AHFP, indicating that the addition of antiseptic stabilizers completely disturbed the process of microbial self-propagation and decay. This is also the essential reason why the changes in both parameters representing microbial characteristics and coagulation behavior of AHFP were different from that of HFP. It is worthy of further study in the near future about the influence of the amount of antiseptic stabilizer addition to AHFP on BGP in this kind of coagulant.

As seen in Fig. 6, HFP gave some essential changes in the colony morphology at 36 d, probably changing into bacilli type, and a small number of bacilli also presented in AHFP at this time. Combined with the changing trend of coagulation behavior (Figs. 1 and 2), it could be inferred that this bacilli type was not suitable for the development of synergistic coagulation action in HFP and AHFP. The colony number and size in HFP and AHFP changed more greatly at 50 d, in comparison with relatively small changes at 45 d: the colony number and size in HFP and AHFP decreased significantly, in which HFP decreased more obviously than AHFP. This indicated that the NOPs in HFP had basically been depleted, resulting in the death of a large amount of microorganisms, probably entering the self-consumption stage completely; while for AHFP, a small amount of NOPs and a large number of microorganisms probably still coexisted, moreover, the coagulation performance was still in the rising phase (Figs. 1 and 2), indicating that the coagulation action of microorganisms in AHFP was dominant at this time and AHFP was still an integrated coagulant composed of NOPs and microorganisms. This was consistent with the above inference. Moreover, according to this trend prediction, the coagulation performance of AHFP maybe still was on the rising trend if the standing time increased continually up to longer 50 d.

The co-coagulation and superposition action consisted of NOPs and microorganisms in this work opened a new perspective for the development and research of an integrated coagulant composed of NOPs and microorganisms, and also provided a probable solution for the instability of microbial coagulants. The coagulation performance by this type of coagulant in treating both simulated HA water and clay water were studied, expanding the water type compared with the previous studies [25], and obtained the conclusion that AHFP gave a strong adaptability to water qualities. However, further research was still needed to other types of water. Therefore, different dominant bacteria groups could be cultivated depending on the specific water qualities to fully exert the synergistic coagulation conducted by both NOPs and microorganisms.

It is worthy of further study about what kind of microorganisms combined with NOPs will be conducive to the co-coagulation or superposition coagulation, and about how the addition ratio of antiseptic stabilizer to AHFP will impact the parameters characterizing BGP in this kind of coagulant. This work probably opened a new thought for the development and research of integrated coagulants composed of NOPs and microorganisms and provided a possibility for making this coagulant an additional carbon source for low-carbon source wastewater treatment.

4. Conclusions

During the entire standing process, both turbidity and color removal by HFP and AHFP all posed some DRCs in treating the simulated HA water and clay water. For the HA water, the turbidity removal by HFP was from 96.7% at 0 d to 69% at 8 d to 79.1% at 10 d to 49.8% at 32 d to 81.6% at 42 d to 59.5% at 45 d to 87.6% at 50 d, and the turbidity removal by AHFP was from 95% at 0 d to 57.9% at 31 d to 86.1% at 36 d to 56.4% at 45 d to 76% at 50 d, respectively.

Sometimes, the DRCs of the parameters characterizing the BGP in HFP and AHFP (such as NOPs, total glycans, pH, and zeta potential) gave a more consistent correspondence with the DRCs of coagulation performance but sometimes did not. This was a proof that this type of coagulants posed a co-coagulation or superposition action performed by both microorganisms and NOPs, moreover, this synergistic coagulation was more complicated. The addition of antiseptic stabilizers to AHFP completely disturbed the process of microorganism self-propagation and decay. Both HFP and AHFP were negatively charged, almost having no neutralization action on pollutants with negative charges. HFP gave very different bacterial morphology from AHFP: the microorganisms in the former presented to be densely dispersed filaments or short lines, and the microorganisms in the latter appeared to be dispersed microbial masses or aggregates. The BGP in HFP was rapid, compared with slow BGP in AHFP, but the BGP in AHFP was larger than that in HFP in the later period.

It is worthy of further study about what kind of microorganisms combined with NOPs will be conducive to the co-coagulation or superposition coagulation, and about how the addition ratio of antiseptic stabilizer to AHFP will impact the parameters characterizing BGP in this kind of coagulants. This work probably opened a new thought for the development and research of integrated coagulants composed of NOPs and microorganisms and provided a possibility for making this coagulant an additional carbon source for low-carbon source wastewater treatment.

Acknowledgments

The authors thank the support of the Teacher Visiting Scholar Funding Project of 2017 funded by University of Jinan (2019–2020).

References

[1] D. Hoornweg, P. Bhada-Tata, C. Kennedy, Environment: waste production must peak this century, Nature, 502 (2013) 615–617.
[2] L.J. Zhu, H.Y. Yang, Y. Zhao, K.J. Kang, Y. Liu, P.P. He, Z.T. Wu, Z.M. Wei, Biochar combined with montmorillonite amendments increase bioavailable organic nitrogen and reduce nitrogen loss during composting, Bioresour. Technol., 294 (2019) 122224, 1–9, doi: 10.1016/j.biortech.2019.12224.
[3] X.Y. Zhao, W.B. Tan, Q.L. Dang, R.F. Li, B.D. Xi, Enhanced biotic contributions to the dechlorination of pentachlorophenol by humus respiration from different compostable environments, Chem. Eng. J., 361 (2019) 1565–1575.
[4] X.Q. Zhao, L. Xiong, M.M. Zhang, F.W. Bai, Towards efficient bioethanol production from agricultural and forestry residues: exploration of unique natural microorganisms in combination with advanced strain engineering, Bioresour. Technol., 215 (2016) 84–91.
[5] M.R. Teixeira, F.P. Camacho, V.S. Sousa, R. Bergamasco, Green technologies for cyanobacteria and natural organic matter water treatment using natural based products, J. Cleaner Prod., 162 (2017) 484–490.
[6] O. Habeeb, R. Kanthasamy, S. Ezzuldin, O.A. Olalere, Characterization of agriculture wastes based activated carbon for removal of hydrogen sulfide from petroleum refinery waste water, Mater. Today: Proc., 20 (2020) 588–594.
[7] L.G.V. Doren, R. Posmanik, F.A. Bicalho, J.W. Tester, D.L. Sills, Prospects for energy recovery during hydrothermal and biological processing of waste biomass, Bioresour. Technol., 225 (2017) 67–74.
[8] L.C. Cao, C. Zhang, H.H. Chena, D.C.W. Tsang, G. Luo, S.C. Zhang, J.M. Chen, Hydrothermal liquefaction of agricultural and forestry wastes: state-of-the art review and future prospects, Bioresour. Technol., 245 (2017) 1184–1193.
[9] N.A. Oladoja, Headway on natural polymeric coagulants in water and wastewater treatment operations, J. Water Process Eng., 6 (2015) 174–192.
[10] N. Zhou, H.G. Chen, Q.J. Feng, D.H. Yao, H.L. Chen, H.Y. Wang, Z. Zhou, H.Y. Li, Y. Tian, X.Y. Lu, Effect of phosphoric acid on the surface properties and Pb(II) adsorption mechanisms of hydrochars prepared from fresh banana peels, J. Cleaner Prod., 165 (2017a) 221–230.
[11] Y.T. Hameed, A. Idris, S.A. Hussain, N. Abdullah, H.C. Man, Effect of pre-treatment with a tannin-based coagulant and flocculant on a biofilm bacterial community and the nitrification process in a municipal wastewater biofilm treatment unit, J. Environ. Chem. Eng., 8 (2020) 103679, 1–7, doi: 10.1016/j.jece.2020.103679.
[12] D.C. Lin, Z.S. Yan, X.B. Tang, J.L. Wang, H. Liang, G.B. Li, Inorganic coagulant induced gypsum scaling in nanofiltration process: effects of coagulant concentration, coagulant conditioning time and fouling strategies, Sci. Total Environ., 670 (2019) 685–695.
[13] Y. Fu, Y.Z. Wang, M.M. Su, Volume and mass reduction of sludge formed by polymerized-organic-Al-Zn-Fe (POAZF) coagulant in treating sewage, Desal. Water Treat., 57 (2016) 6239–6249.
[14] Y. Fu, D. Gao, X. Yu, A combined process of "short-time coagulation-sedimentation-filtration": behavior and mechanism

of poly-Si-Fe (PSF) coagulant, Desal. Water Treat., 171 (2019) 314–324.
[15] X.J. Hu, X.B. Zhang, H.H. Ngo, W.S. Guo, H.T. Wen, C.C. Li, Y.C. Zhang, C.J. Ma, Comparison study on the ammonium adsorption of the biochars derived from different kinds of fruit peel, Sci. Total Environ., 707 (2020) 135544, 1–9, doi: 10.1016/j.scitotenv.2019.135544.
[16] T.A. Sial, M.N. Khan, Z. Lan, F. Kumbhar, Z. Ying, J.G. Zhang, D.Q. Sun, X. Li, Contrasting effects of banana peels waste and its biochar on greenhouse gas emissions and soil biochemical properties, Process Saf. Environ. Prot., 122 (2019) 366–377.
[17] P. Khawas, A.J. Das, K.K. Dash, S.C. Deka, Thin-layer drying characteristics of kachkal banana peel (Musa ABB) of Assam, India, Int. Food Res. J., 21 (2014) 1011–1018.
[18] V.M. Komal, K.R. Virendra, Utilization of banana peels for removal of strontium(II) from water, Environ. Technol. Innovation, 11 (2018) 371–383.
[19] A.E. Nemr, O. Abdelwahab, A. El-Sikaily, A. Khaled, Removal of direct blue-86 from aqueous solution by new activated carbon developed from orange peel, J. Hazard Mater., 161 (2009) 102–110.
[20] A. Ali, K. Saeed, Phenol removal from aqueous medium using chemically modified banana peels as low-cost adsorbent, Desal, Water Treat., 57 (2015) 11242–11254.
[21] J. Ma, S.S. Sun, K.Z. Chen, Facile and scalable synthesis of magnetite/carbon adsorbents by recycling discarded fruit peels and their potential usage in water treatment, Bioresour. Technol., 233 (2017) 110–115.
[22] A. Cabral-Prieto, Orange peel+nanostructured zero-valent-iron composite for the removal of hexavalent chromium in water, Renewable Sustainable Energy Rev., 70 (2017) 814–821.
[23] V.S. Munagapati, Adsorption of anionic azo dye congo red from aqueous solution by cationic modified orange peel powder, J. Mol. Liq., 220 (2016) 540–548.
[24] N. Zhou, H.G. Chen, J.T. Xi, D.H. Yao, Z. Zhou, Y. Tian, X.Y. Lu, Biochars with excellent Pb(II) adsorption property produced from fresh and dehydrated banana peels via hydrothermal carbonization, Bioresour. Technol., 232 (2017b) 204–210.
[25] Y. Fu, X.J. Meng, N.N. Lu, H.L. Jian, Y. Di, Characteristics changes in banana peel coagulant during storage process, Int. J. Environ. Sci. Technol., 16 (2019) 7747–7756.
[26] H. Salehizadeh, N. Yan, Recent advances in extracellular biopolymer flocculants, Bioresour. Technol., 32 (2014) 1506–1522.
[27] Z. Li, R.W. Chen, H.Y. Lei, Z. Shan, T. Bai, Q. Yu, H.L. Li, Characterization and flocculating properties of a novel bioflocculant produced by *Bacillus circulans*, World J. Microbiol. Biotechnol., 25 (2009) 745–752, doi: 10.1007/s11274-008-9943-8.
[28] S.P. Buthelezi, A.O. Olaniran, B. Pillay, Textile dye removal from wastewater effluents using bioflocculants produced by indigenous bacterial isolates, Molecules, 17 (2012) 14260–14274.
[29] Y.H. Wang, R.Q. Liu, W.F. Liu, L.B. Tong, Q.W. Wang, R.N. Wang, Production of a Novel Bioflocculant by Culture of Pseudomonas Alcaligenes Using Brewery Wastewater and Its Application in Dye Removal, 2009 International Conference on Energy and Environment Technology, Guilin, Guangxi, China, 2009.
[30] H. Salehizadeh, N. Yan, R. Farnood, Recent advances in polysaccharide bio-based flocculants, Biotechnol. Adv., 36 (2018) 92–119.
[31] Y.X. Wang, Study on Biofilocculation-Producing Origin of *Ruditapes philippinarum* Coagulation Mud Based on Microbiome, Master's Thesis, Zhejiang Ocean University, Hangzhou, 2019 (in Chinese).
[32] M. Shahadat, T.T. Teng, M. Rafatullah, Z.A. Shaikh, T.R. Sreekrishnan, S.W. Ali, Bacterial bioflocculants: a review of recent advances and perspectives, Chem. Eng. J., 328 (2017) 1139–1152.